

PN, PS Mass Concentrations and PN/PS Ratio (2007 – 2023)

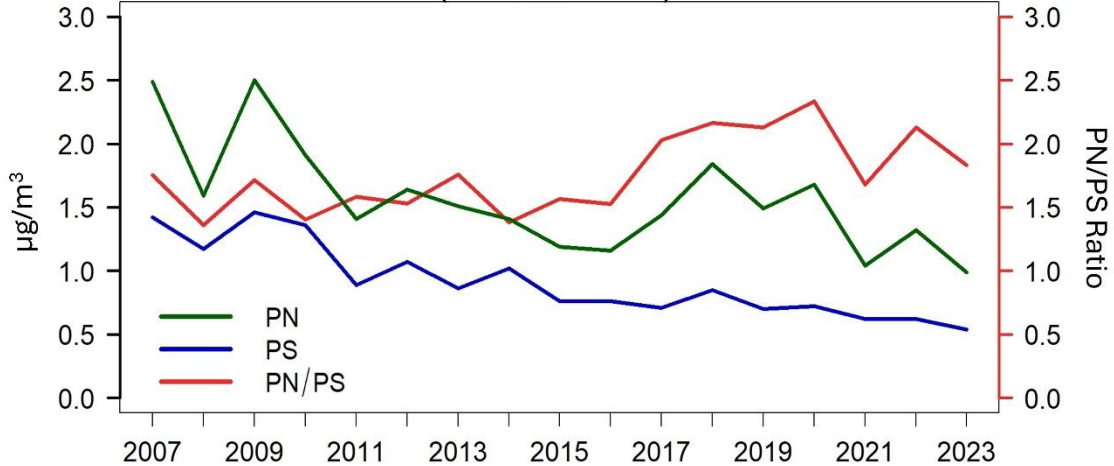


Figure S1: Wintertime PN mass concentrations (green), PS mass concentrations (blue), and PN/PS ratios (in red) over the MWUS from 2007 to 2023.

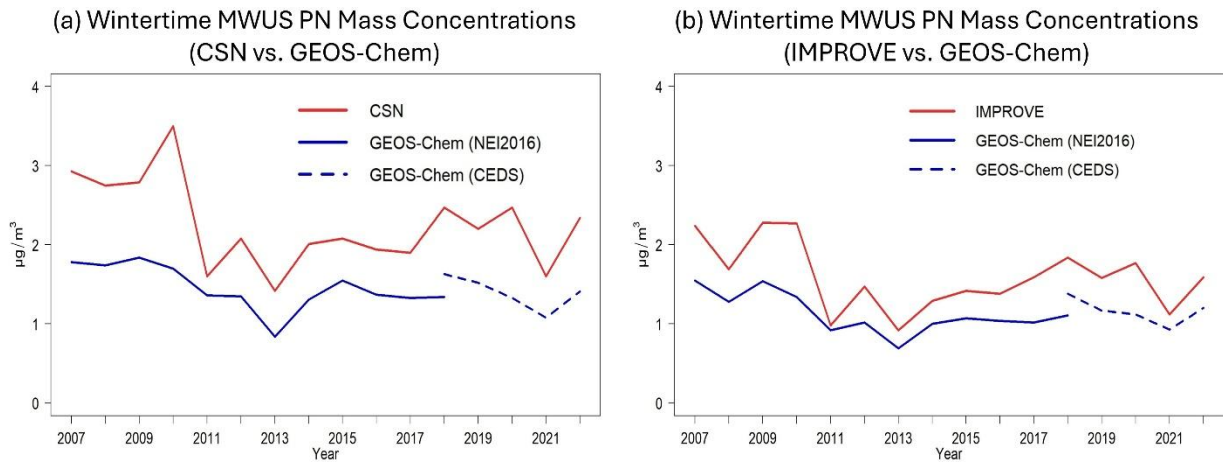


Figure S2: The comparisons in wintertime PN trends between ground monitoring observations, (a) CSN and (b) IMPROVE, and the Base simulation in GEOS-Chem. Solid red lines represent the wintertime PN mass concentrations from ground monitoring observations (IMPROVE and CSN). Solid blue lines represent the wintertime PN mass concentrations from GEOS-Chem using NEI2016 emissions inventory. Dashed blue lines represent the wintertime PN mass concentrations from GEOS-Chem using CEDS emissions inventory.

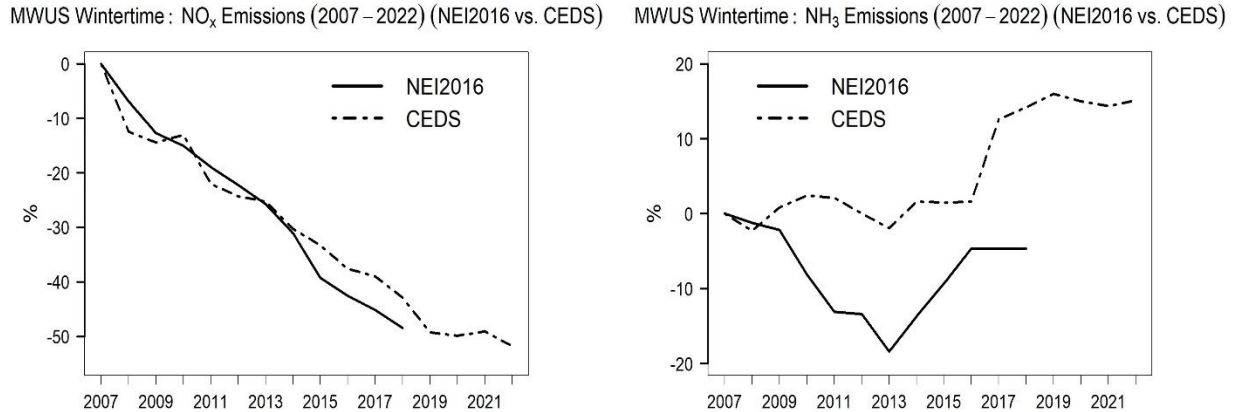


Figure S3: Wintertime NO_x emissions (left) and NH₃ emissions (right) using NEI2016 emissions inventory (solid lines) and CEDS emissions inventory (dashed lines and points) over the MWUS (2007–2022).

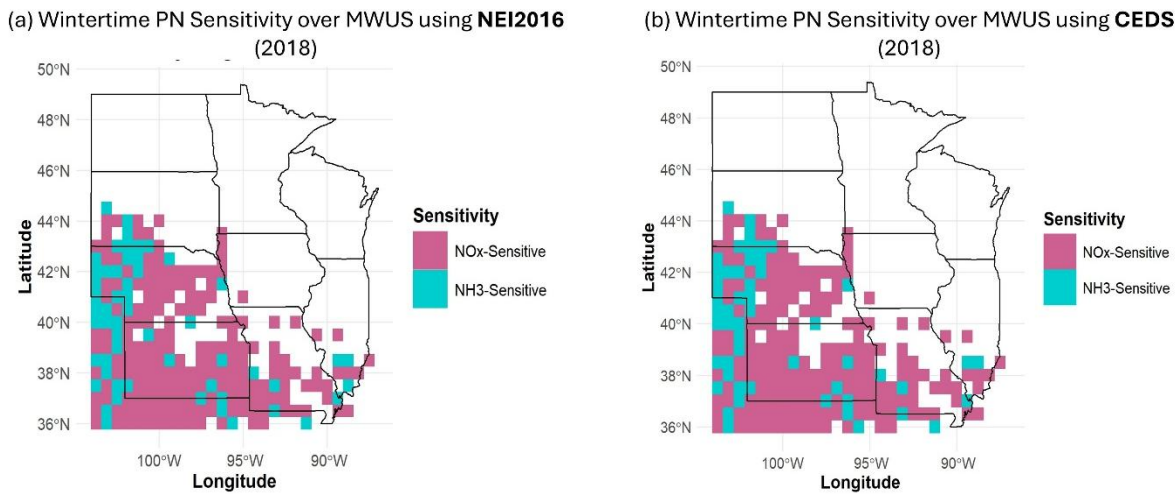


Figure S4: Wintertime PN sensitivity in winter 2018 (i.e., Jan 2019) using NEI2016 emissions inventory (left) and CEDS emissions inventory (right). Pink pixels indicate PN formation is sensitive to NO_x emissions (i.e., NO_x-sensitive), and blue pixels indicate PN formation is sensitive to NH₃ emissions (i.e., NH₃-sensitive).

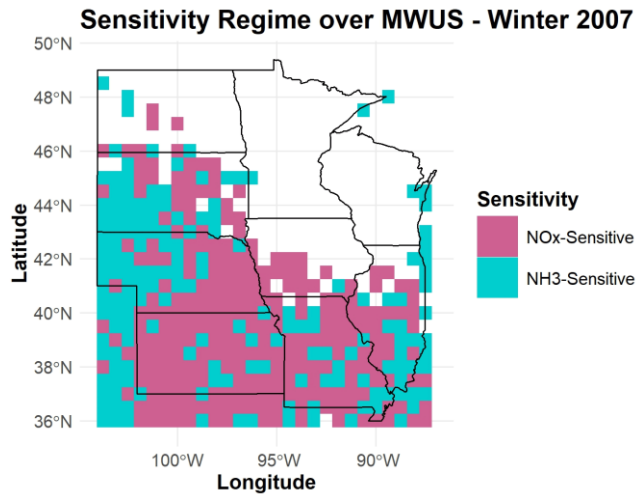


Figure S5: The distribution of wintertime PN sensitivity regime over MWUS (2007 – 2023). Pink pixels indicate PN formation is sensitive to NO_x emissions (i.e., NO_x-sensitive), and blue pixels indicate PN formation is sensitive to NH₃ emissions (i.e., NH₃-sensitive).

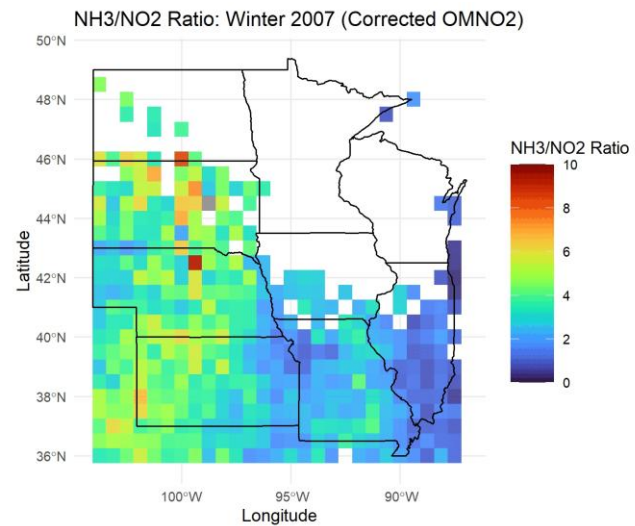


Figure S6: The distribution of wintertime satellite tropospheric column NH₃/NO₂ ratios over MWUS (2007 – 2023). Grey pixels indicate NH₃/NO₂ ratios > 10.

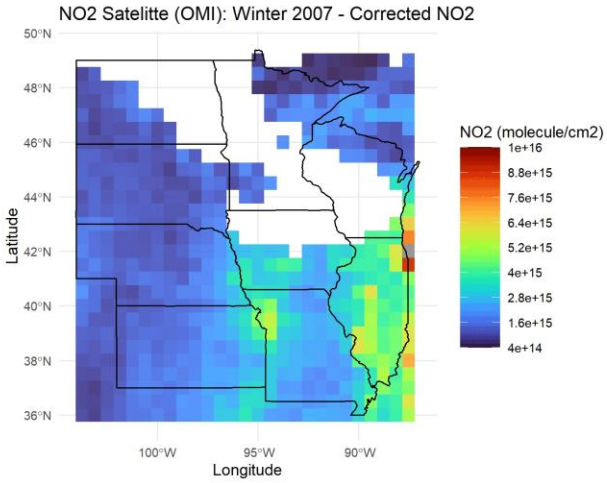


Figure S7: The distribution of wintertime NO₂ column density (2007 – 2023) over MWUS. Warmer color indicates higher NO₂ column densities, and colder color indicates lower NO₂ column densities. Grey pixels indicate NO₂ column density $> 1 \times 10^{16}$ molecules cm⁻².

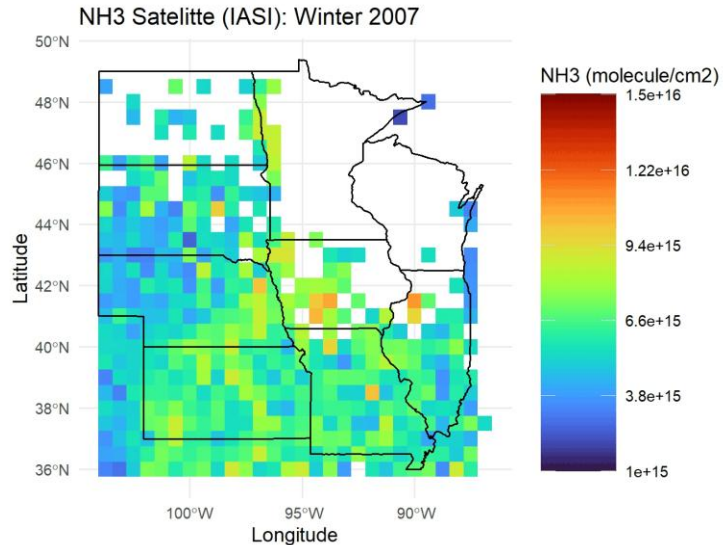


Figure S8: The distribution of wintertime NH₃ column density from IASI (2007–2023) over MWUS. Warmer color indicates higher NH₃ column densities, and colder color indicates lower NH₃ column densities. Grey pixels indicate NH₃ column density $> 1.5 \times 10^{16}$ molecules cm⁻².

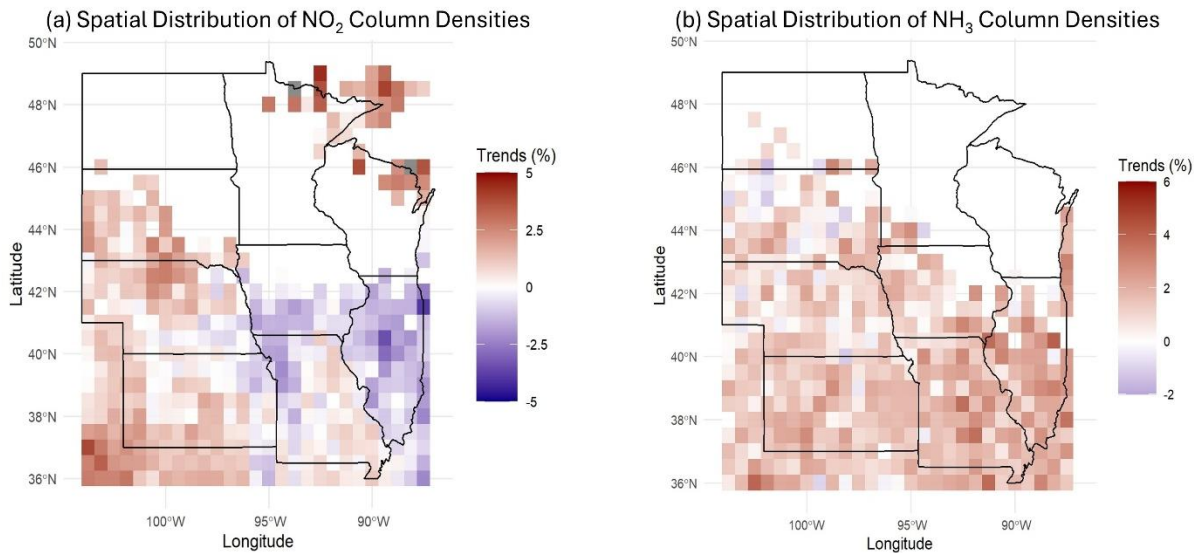


Figure S9: The spatial trends of wintertime (a) NO_2 and (b) NH_3 column density over MWUS (2007–2023). The increasing trend of NO_2 and NH_3 column densities is shown in red, and the decreasing trend in NO_2 and NH_3 column densities is shown in blue. Grey pixels indicate an increase $> 5\%$ in NO_2 column density for panel (a) only.

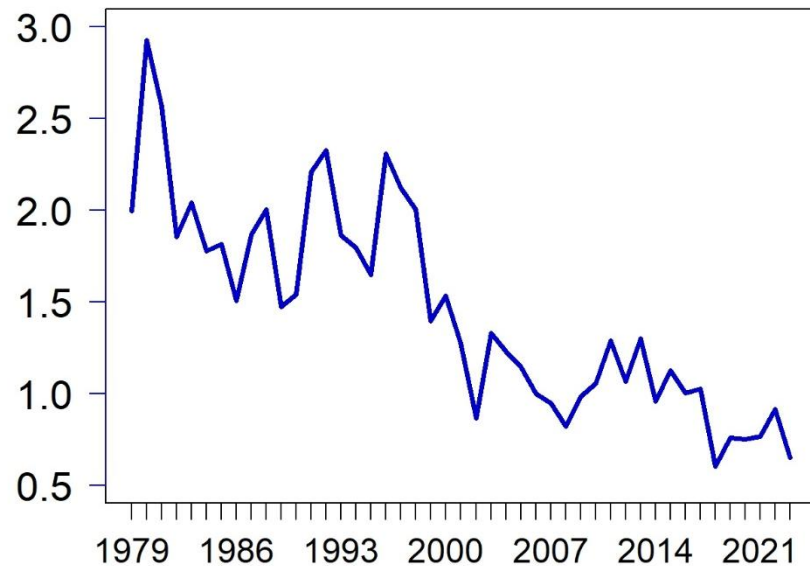


Figure S10: Wintertime nitrate wet deposition (NWD) trends over the MWUS from 1979 to 2023 using the National Trends Network.

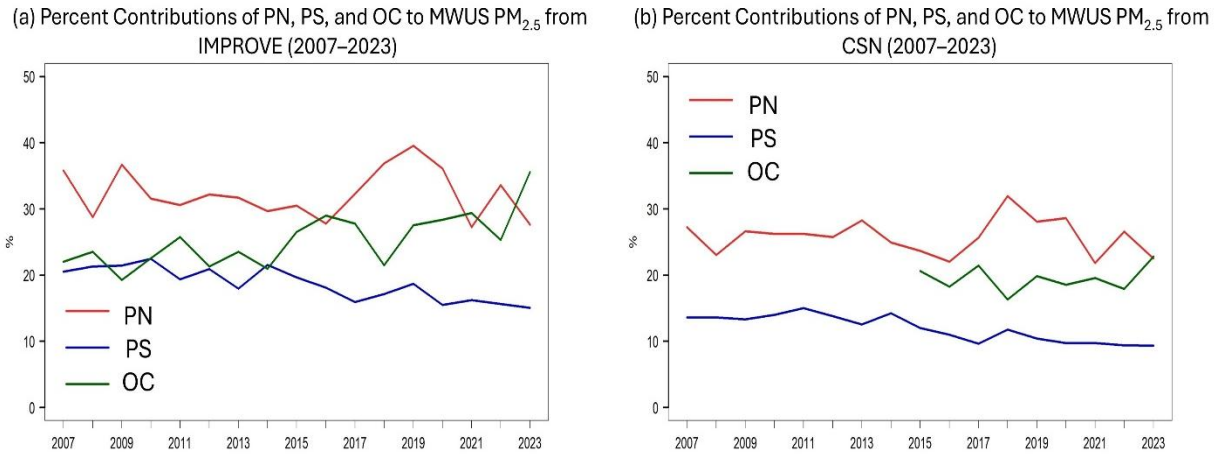


Figure S11: The contributions of PN (red), PS (blue), and total organic carbon (OC) (green) to total $\text{PM}_{2.5}$ trends over the MWUS (2007 – 2023) using (a) IMPROVE and (b) CSN ground monitoring observations.

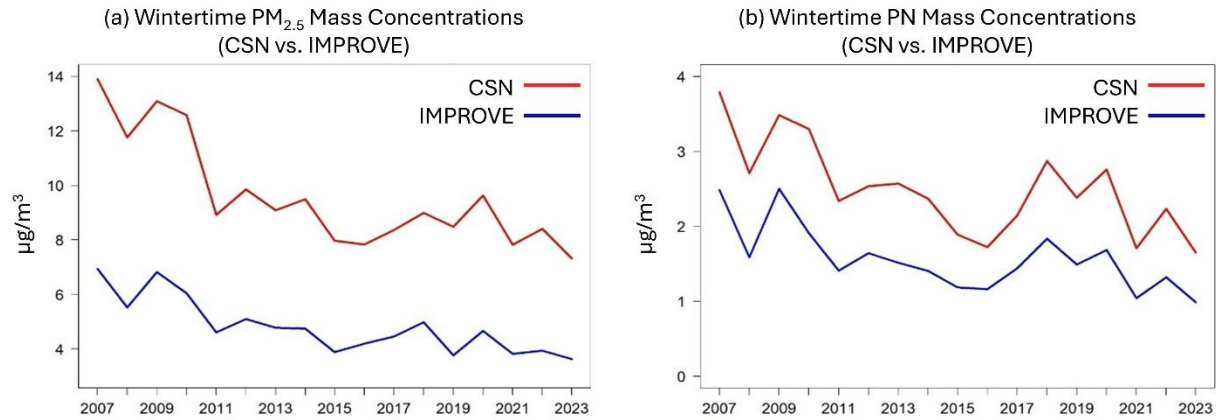


Figure S12: Wintertime $\text{PM}_{2.5}$ and PN trends over urban and rural areas in MWUS (2007 – 2023) using IMPROVE (blue) and CSN (red) ground monitoring observations.